Land Use and Land Cover Analyses from the North Coast of Puerto Rico Using AVIRIS Images: from Arecibo to Quebradillas

Diana C. Prado Garzon[1], Gian Villamil[2]

[1]*Undergraduate student – Department of Geology*

[2]*Undergraduate student – Department of Physics*

University of Puerto Rico, Mayaguez Campus

ABSTRACT.- Using images of the Airborne Visible Infrared Imaging Spectrometer (AVIRIS) instrument it is possible to analyze the spectral bands to produce a land use and land cover map of the north coast of Puerto Rico. Using various steps of preprocessing including two different types of atmospheric correction a Region of Interest map was created to submit the image to supervised and unsupervised classification. Results showed that a supervised classification using maximum likelihood is the most successful way to categorize the area of study into the desired categories. However not one method was error free as some confused various parameters. It was also shown that the dark subtract method of atmospheric correction is better than QUick Atmospheric Correction.

KEYWORDS**. -** AVIRIS, Atmospheric Correction, Hyperspectral Sensor, Spectral Subset, Land Use, Land Cover, Supervised Classification, Unsupervised Classification

INTRODUCTION

Image spectroscopy is the practice that collects images with a sensor that measures the energy that reaches each element of spatial resolution in the image. It is based on molecular absorption and reflectance characteristics from the different materials. This new tool is used to map specific material by detecting specific chemical bonds, thus, making it an excellent tool for environmental assessments, mineral mapping and exploration, classification of vegetation communities and species, health studies and land management (Fig.1) (usgs.com).

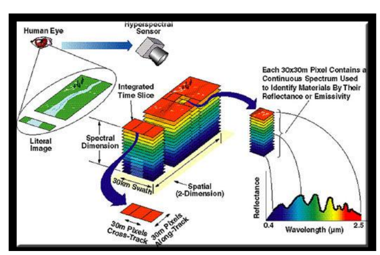

Fig 1. Image spectroscopy concept. (http://www.eoc.csiro.au/hswww/HS_concept3.jpg)

According to NASA, an image spectrometer is an object designed to detect, measure and analyze the spectral content from the incident radiomagnetic radiation upon an object. An example of this instrument is the Airborne Visible Infrared Imaging Spectrometer (AVIRIS) sensor (Figs. 2 & 3). This sensor has 224 bands and it is installed in the airborne platform ER-2; it has a spectral range between 400 – 2450 nm, a spatial resolution of 20 km and a swath width of 10.5 km. Its spectral resolution is 1 nm and its spectral coverage is continuous (Hirano et al., 2003).

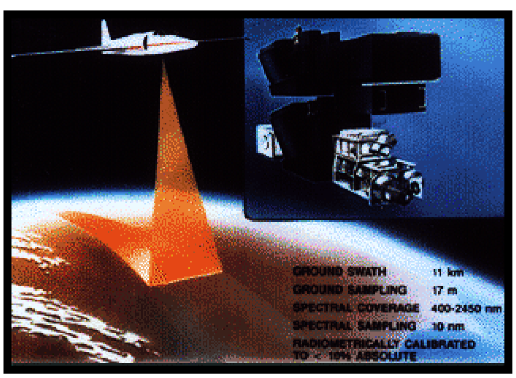

Fig 2. Airborne platform ER-2. (http://aviris.jpl.nasa.gov/html/av_swath_shadow.gif)

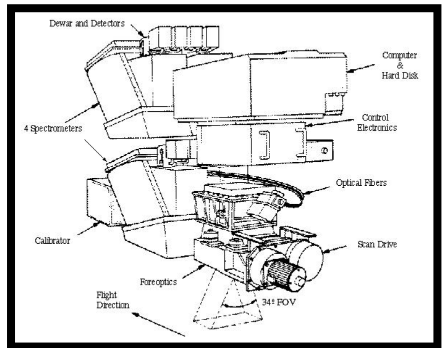

Fig 3. AVIRIS Instrument. (http://www.eoportal.org/directory/images/Aviris_At_Anchor0.jpeg)

Clark et al. (2002) demonstrated the usefulness of AVIRIS in the identification of surface minerals for map development. Their study included acidic rocks drainage, vegetation species, better understanding of geologic processes such as fault detection, weathering, mineralization, hydrothermal alterations, etc. Figures 4 – 7 show their results. Other studies include Mars and Crowley (2003), who used AVIRIS to map mine waste dumps, wetlands vegetation, and other applications in southeastern Idaho; Schellberg et al. (2008) and Clevers (2009) who used image spectrometry in agricultural applications. Other possible applications of AVIRIS include atmospheric studies, ecology, soils, water bodies, mining, etc.

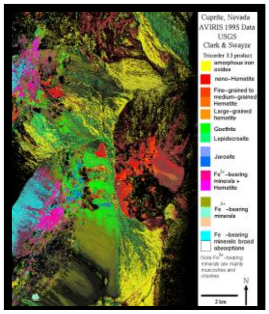

Fig 4. Cuprite, Nevada AVIRIS 1995 data (after Clark et al., 2002).

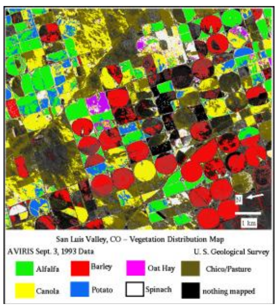

Fig 5. Agriculture distribution map from San Luis Valley, Colorado. (after Clark et al., 2002).

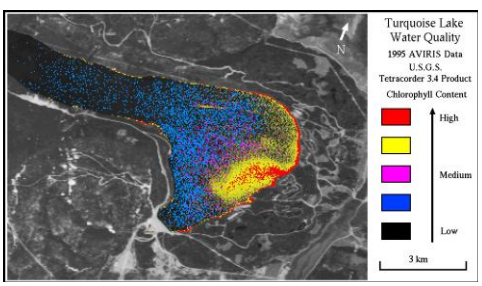

Fig 6. Turquoise Lake water quality 1995 AVIRIS data (after Clark et al., 2002).

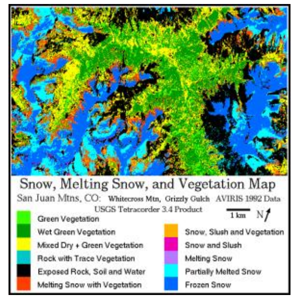

Fig 7. Snow and vegetation cover from the San Juan mountains, Colorado (after Clark et al., 2002).

On August 19th, 2004, the ER-2 from NASA Ames Research Center covered the area of Puerto Rico. The platform carried three sensors: the Wild Heerbrugg RC-10, AVIRIS and Cirrus Digital Camera System (DCS). Figures 8 and 9 show the path of the aircraft. The aircraft started covering the north coast are of Puerto Rico at 14:40 and ended at 14:56 (GMT time).

Fig 8. Aircraft path mission (courtesy of Dr. Gilbes)

Fig 9. Checkpoints (courtesy of Dr. Gilbes)

MATERIALS AND METHODS

In order to properly analyze the images, certain steps in preprocessing were needed. The first of them was to create a subset of the main image (Fig. 10) and to flip the generated image in order to focus our study in a specific region between Quebradillas and Arecibo (Fig. 11) or more specifically from the coordinates 66º 56'W to 66º 37'W and from 18º 27'N to 18º 32'N.

After the region of study is generated it is necessary to also create a spectral subset since the sensor AVIRIS is a hyperspectral one and for our study some of the bands generated by AVIRIS are useless.

Fig 10. Original image taken by AVIRIS

Fig 11. Region of Study of the north coast of Puerto Rico

The spectral subset is done by generating several z-spectrums (Fig 12) of various features in the image and eliminating the regions of high absorbency.

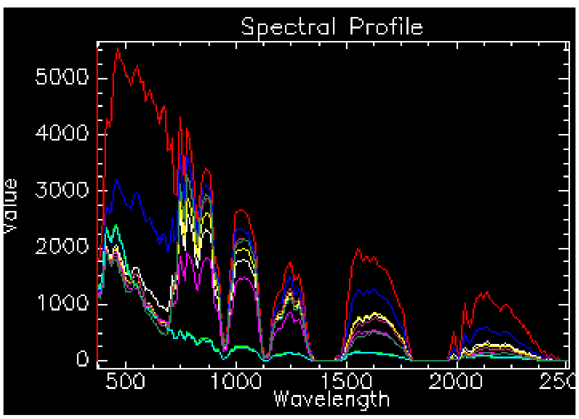

Fig 12. Spectral profiles of various features

This step is crucial since the main purpose is to eliminate the lowest minimum band value that is useless in our study.

However, as it will be seen later, even with doing a spectral subset, errors can occur. The next step in the pre-processing is the atmospheric correction. Here the dark subtract method was used using the band minimum as the subtract method. The generated image was then compared to the original to see if the atmospheric correction worked. This is seen by comparing each digital value (DV) since the dark subtract DVs should be less than the original image DVs. The dark subtract image led to higher than supposed DVs therefore another method of atmospheric correction called QUick Atmospheric Correction (QUAC) was used until the pixel containing the error in DV was found and fixed. In order to find the error containing pixel, an unsupervised classification was made as an attempt that ENVI would classify as a separate class altogether (figure not shown). Once the pixel was found, another spatial subset was made (Fig. 13).

Fig 13. Shows the region eliminated from the study in order to eliminate the pixels containing the error in Digital Value.

Pixel	Without Atm. Correction			QUick Atm. Correction			Dark Substract		
before	R	G	B	R	G	B	R	G	B
1	858	1774	1989	377	402	93	4482	5398	5616
2	598	1117	2254	186	137	156	4222	4741	5878
3	1692	2156	2586	987	557	235	5316	5780	6210
4	803	1161	1984	336	155	92	4427	4785	5608
5	7848	9429	10400	5497	3493	2082	11472	13053	14024

Pixel	Without Atm. Correction			QUick Atm. Correction			Dark Substract		
after	R	G	B	R	G	B	R	G	B
1	611	1118	2241	196	138	153	267	357	647
2	1209	1860	2133	634	437	127	865	1099	539
3	698	1113	1977	259	136	91	354	352	383
4	9522	11326	12379	6723	4258	2550	9178	10565	10785
5	557	1140	1783	156	147	45	213	379	189

Table 1. Comparison of Digital values of each method of atmospheric correction before and after the error containing pixel was found.

After the region of study was again spatially subset, it was submitted to another dark subtract atmospheric correction. Table 1 shows the comparison of DVs before and after the pixel was found.

Once all of the pre-processing was finished in order to properly classify the image various regions of interest (ROI) were needed. The ROIs were chosen according to various features seen on the image. They were: highways, clouds, rivers, sand, ocean, vegetation, deforested areas, and urban areas. Figure 14 shows the ROIs selected for the region of study. After the ROI file was created, the next step was to proceed with the classification of the image. For this part,

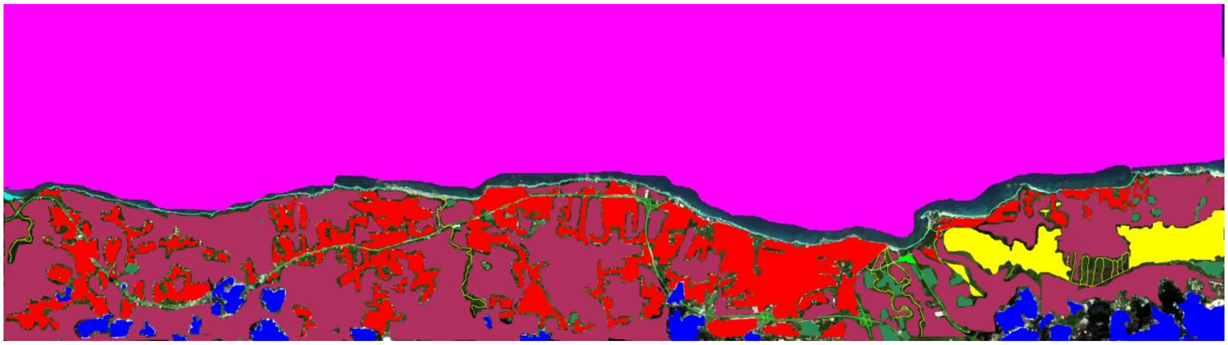

Fig 14. ROI map created for the classifications

an unsupervised classification and a supervised classification was made to the image corrected by dark subtract and by QUick Atmospheric Correction in order to determine which atmospheric correction works best. For the unsupervised classification the methods used were K-means and Isodata and for the supervised classifications the methods used were the minimum distance and maximum likelihood. The numbers of classes used for the unsupervised and supervised classifications was eight and the numbers of iterations used for the supervised classification was three.

RESULTS AND DISCUSSION

For unsupervised classifications, Isodata provided better classifications in urban areas and what we think were shallow water for the Dark Subtract atmospheric corrected image. It also identified clouds and their shadows in both atmospheric corrections (Figs. 15 & 16). K-means unsupervised classification tried to identify the clouds as a separate class in the Dark Subtract atmospheric corrected image, but in general, its results are very similar to the Isodata classification (Figs. 17 & 18).

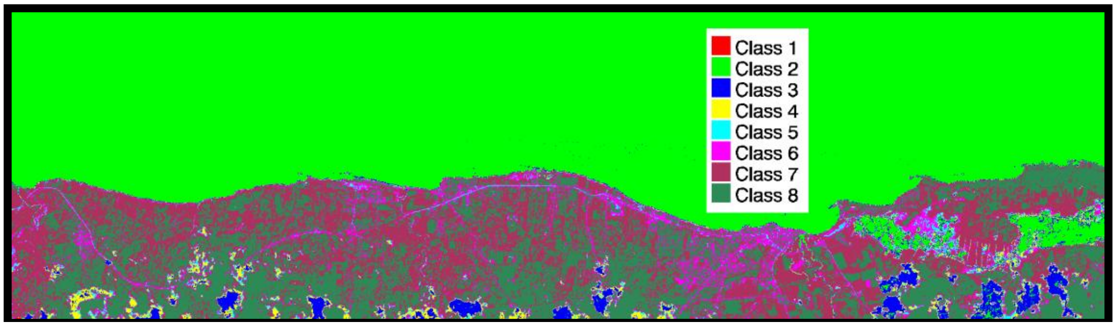

Fig 15. Unsupervised classification Isodata (quick atmospheric corrected image).

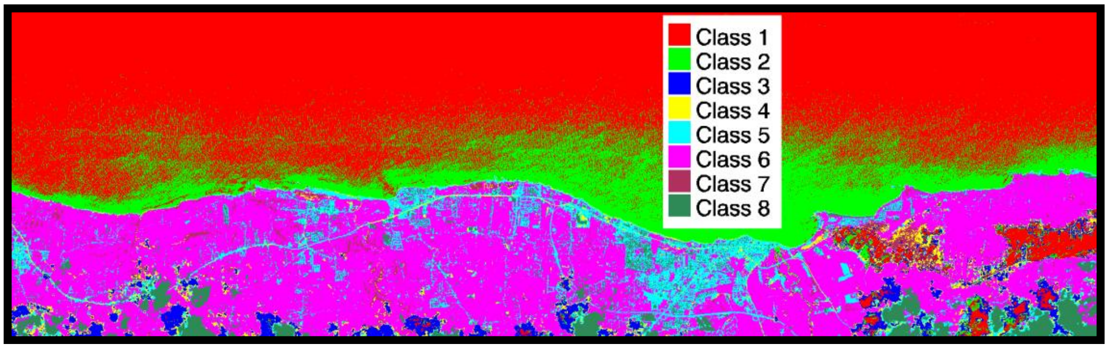

Fig 16. Unsupervised classification Isodata (dark substract image).

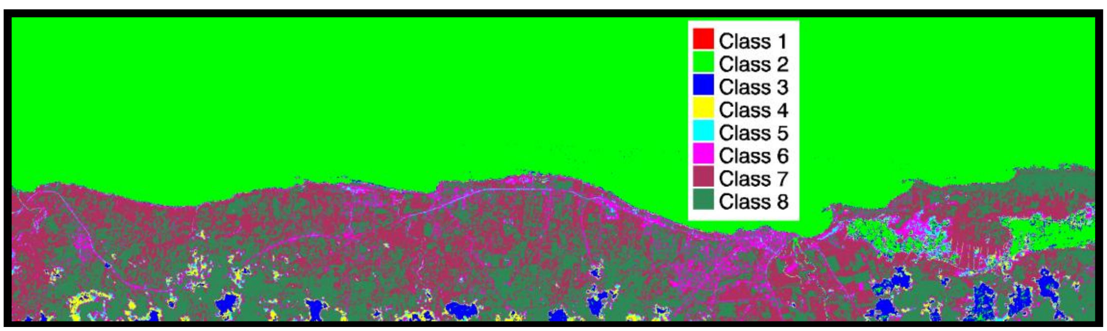

Fig 17. Unsupervised classification K-means (quick atmospheric corrected image).

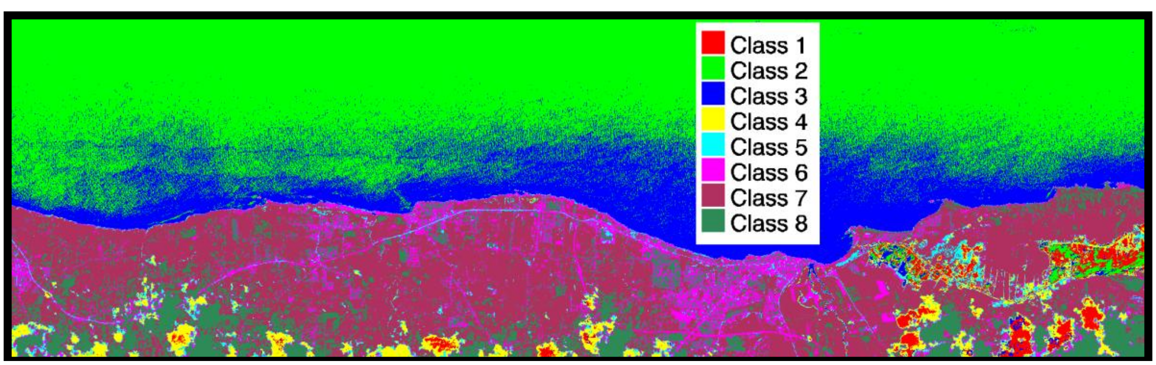

Fig 18. Unsupervised classification K-means (dark substract image).

For supervised classifications, the quick atmospheric corrected image identified erroneously rivers as if they were ocean in the Minimum Distance classification; the rest of the classifications were identified correctly. As for Maximum Likelihood, all classifications were correct, but the dark substract image seemed to show what seemed to be shallow waters (Figs. 19 - 22). When compared to bathymetry data, we observed that this class is not due to shallow water, but to roughness of water (Fig. 23). No Neural Net classification was possible due to the need of better processing capacity; we needed a faster computer. We understand that the problem is due to the high amount of spectral bands. Overall, we observed that amongst the two different atmospheric corrections, dark subtract allows to obtain better results. The best classification was the Maximum Likelihood classification.

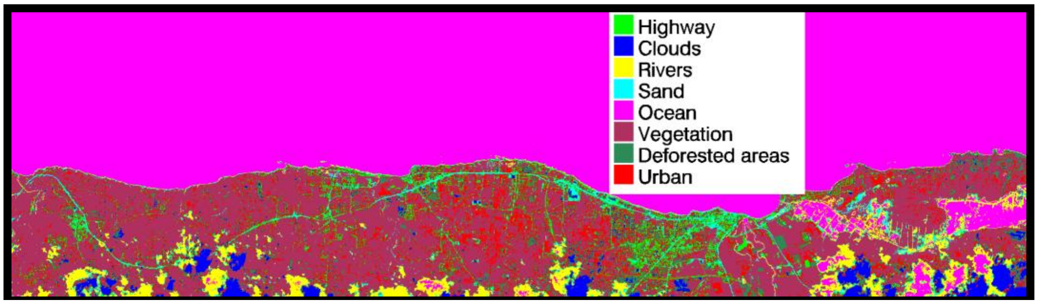

Fig 19. Supervised classification Minimum Distance (quick atmospheric corrected image).

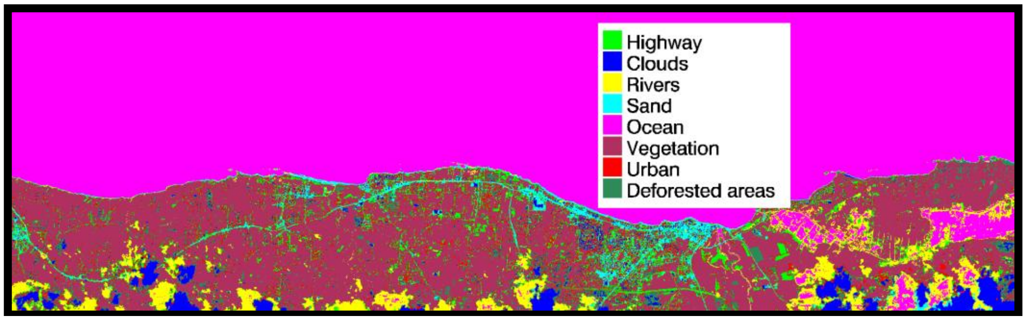

Fig 20. Supervised classification Minimum Distance (dark substract image).

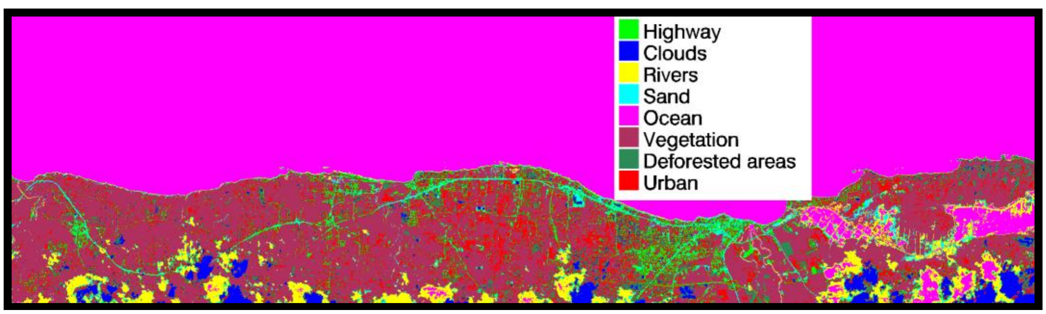

Fig 21. Supervised classification Maximum Likelihood (quick atmospheric corrected image).

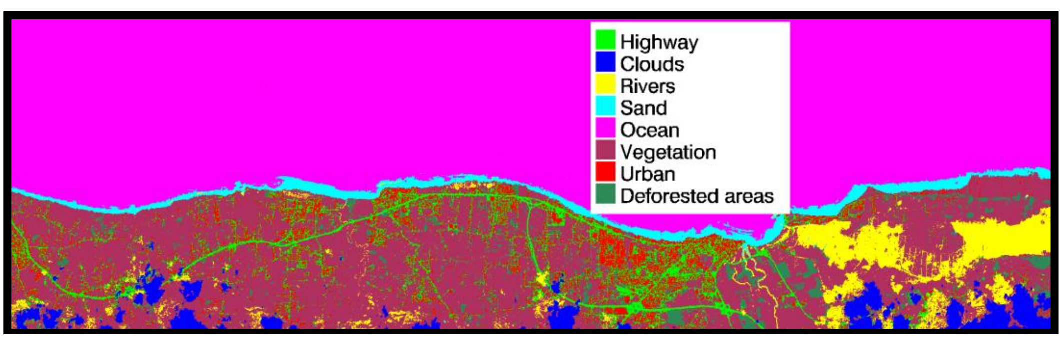

Fig 22. Supervised classification Maximum Likelihood (dark substract).

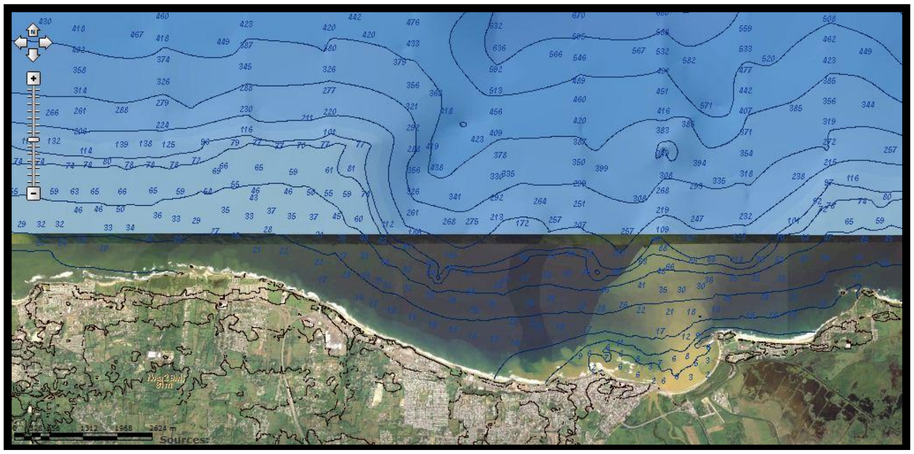

Fig 23. Bathymetric map of the area of study. (http://gis.otg.gobierno.pr/maptest/)

ACKNOWLEDGEMENTS

We would like to thank our families for their unconditional support throughout our research, Dr Gilbes for providing the AVIRIS raw images and our classmates for their support as well.

REFERENCES

Clark, R. N., G. A. Swayze, K. E. Livo, R. F. Kokaly, S. J. Sutley, J. B. Dalton, R. R. McDougal, and C. A. Gent, Imaging spectroscopy: Earth and planetary remote sensing with the USGS Tetracorder and expert systems, *J. Geophys. Res., 108(E12), 5131, doi:10.1029/2002JE001847, pages 5-1 to 5-44, December, 2003.* [*http://speclab.cr.usgs.gov/PAPERS/tetracorder*](http://speclab.cr.usgs.gov/PAPERS/tetracorder).

Clevers, J.G.P.W., 1999, The use of imaging spectrometry for agricultural applications: Journal of Photogrammetry & Remote Sensing, v.54, pp. 299 – 304.

Mars, J.C., Crowley, J.K., 2003, Mapping mine wastes and analyzing areas affected by selenium-rich water runoff in southeast Idaho using AVIRIS imagery and digital elevation data: Remote Sensing of Environment, v. 84, pp. 422 – 436.

Schellberg, J., Hill, M.J., Gerhards, R., Rothmund, M., Braun, M., 2008, Precision agriculture on grassland: Applications, perspectives and constraints: European Journal of Agronomy, v. 29, pp. 59 – 71.